



Design of optimized energy system based on active energy-saving technologies in very low-energy smart buildings

Affaq Qamar¹ | Javed Iqbal² | Saim Saher¹ | Arif Ali Shah³ | Abdul Basit¹

¹Center for Advanced Studies in Energy, University of Engineering and Technology Peshawar, Peshawar, Pakistan

²Sarhad University of Information Technology, Peshawar, Pakistan

³Department of Electrical Engineering, Abasyn University Peshawar, Peshawar, Pakistan

Correspondence

Javed Iqbal, Sarhad University of Information Technology, Peshawar, Pakistan.
Email: javed.iqbal@ieeepk.edu.pk

Abstract

The International Energy Agency proclaims that the energy utilization by commercial buildings makes up 28% of the world's total energy consumption. This research is aimed at finding various optimum ways to minimize energy consumption for existing commercial buildings. A three-layer framework is proposed to achieve active energy saving and to transform an existing building into very low-energy building. The building considered is the postgraduate studies research lab that can have 15 workstations. The building site (envelop) is made scalable by dividing the site area into zones and each zone is monitored via a sensor node, which monitors occupant behavior and acts as a controlling agent between the source and the load. The use of photovoltaic as renewable generation is a sustainable and environment-friendly way and thus, is added to the existing building to conserve energy. A 6 kW grid-tied monocrystalline photovoltaic-based renewable energy system has been added to the building to meet energy requirements and envisage its aftereffect on the energy conservation. The energy-efficient appliances have been used as loads to minimize the energy consumption. The installed system has a payback period of 6 years, while the proposed framework can achieve maximum energy efficiency of 90%.

1 | INTRODUCTION

Energy is utilized as a part of structures to convey agreeable conditions for tenants and to control machines, ie, this is known as “in-use energy.” Energy is additionally utilized in the manufacturing of building materials and also in construction process: this is known as “embodied energy.” Right now, the energy being used over the lifetime of most structures significantly surpasses their embodied energy.¹ Energy efficiency in existing buildings is one of a crucial requirement of the 21st century. Several strategies and methodologies of retrofits involving information and communication technologies (ICT) technologies are now being implemented in the modern building designs. As a preinvestigation, computer-aided design tools are employed to see impacts and energy saving because of specific technologies. This is also helpful in measuring the efficiency in energy consumption of specific housing with microscale refurbishment strategies. The integration of renewable energy technologies and building renovation are the two key procedures for improving energy sustainability of buildings at a neighborhood scale. The proposed work accounts for transformation of an existing building space into energy-efficient building by integrating following active energy-saving techniques:

- Power-saver schemes,
- Energy generation via renewable,

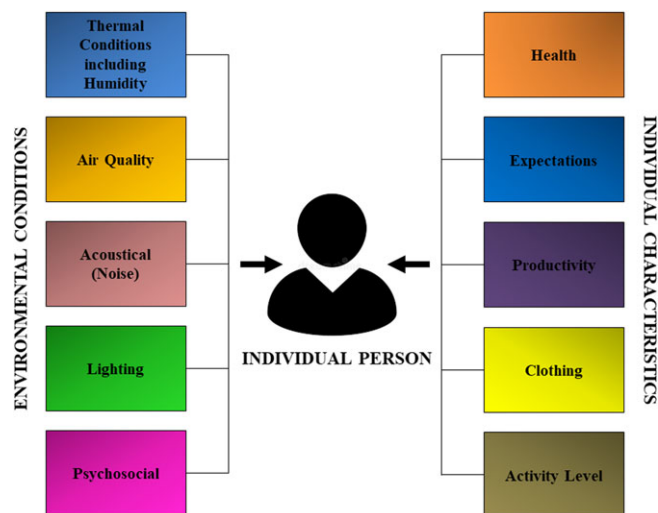


FIGURE 1 Personal environment model

- Energy efficient/smart lighting,
- Smart load monitoring and management.

The building space selected as a case study is to be used as a faculty office of Abasyn University located in Peshawar, Pakistan. The transformation into an energy-efficient building must ensure that the human comfort is achieved. Human comfort or thermal comfort is a term related to the air quality and surrounding conditions that are generally liked by human beings and make them feel comfortable as depicted in Figure 1. These are usually dependent on temperature, humidity, air movement and freshness, noise, lighting etc.² The general temperature range is 20 to 25°C with 30% to 60% relative humidity with respect to the season. Even for low-energy and energy-saver techniques, human comfort cannot be compromised and at least minimal levels should be attained for uncomfortable environment, for it can adversely affect the health and productivity of the people. These factors are undesirable, especially in a workplace.

2 | LITERATURE REVIEW

The literature offers a great number of methodologies and tools aimed at improving energy efficiency of existing buildings. Each methodology has its specific base hypothesis and could obtain different temporal details based on proposed methodology.

The research conducted by Heidari et al³ suggested that lighting energy consumption in the household can be decreased cost-effectively from 5.4 PJ today to 2 PJ (−62%) by year 2035 with a payback period of less than two years, thanks to replacing incumbent bulbs with highly energy-efficient LED technology. An intelligent energy management for premises with no set occupant pattern has always been a challenging scenario. A novel methodology has been proposed in the work of Raftery et al,⁴ with an effort to keep it compatible with any existing energy management infrastructure of a building. This involves estimation of energy cost for air conditioning appliances at three different supply air temperatures (current, higher, and lower), and chooses the one with the lowest cost as the set point. The proposed strategy resulted in cost reduction of Heating Ventilation Air Conditioning (HVAC) by 29% as compared to industrial standard energy management control methods.

The monitoring data give evidence of a statistically significant relationship between perceived control and the thermal sensations of occupants.⁵ Dynamic building energy simulations shows that increasing occupants' perceived level of control over the thermal environment could reduce cooling energy consumption by 9% without sacrificing the thermal comfort of the occupants. The utilization of comprehensive fine-grained occupancy information is also very vital in the efficient application of demand-driven measures in buildings. This was achieved by embedding pressure sensors in office chairs to collect location data of occupants within office area.⁶ Yoganathan et al⁷ have used cluster analysis using partition- and density/spatial-based algorithms, which uses Pareto principle to derive the optimal number and locations of sensors. The results indicate that the total number of sensors can be reduced to 20% (ie, from 31 to 6 sensors) with minimal information loss using the proposed techniques as compared to heuristic placement strategies.

The research in the work of Li and Dong⁸ developed a new moving-window inhomogeneous Markov model based on change point analysis, which outperforms the other methods with a max 22% difference in terms of presence forecasts

Implementation	Energy-efficient technologies	kWh savings
Heidari et al ³	Energy-Efficient Lighting	62%
Rafferty et al ⁴	Energy-Efficient Infrastructure for HVACs	29%
Labeodan et al ⁶	Occupant perceived control as load management	9%
Zou et al ⁹	Occupancy driven light control	80%
This paper	DG + Energy-Efficient Loads + Intelligent Load Mgt.	90%

TABLE 1 Energy efficiency comparison

Abbreviations: DG, distributed generation.

for 15 minutes, 30 minutes, and 1 hour ahead. The proposed Markov model also outperforms other models in occupancy number prediction for all forecast windows with 0.34 root mean square error and 0.23 mean absolute error, respectively. Zou et al presented WinLight,⁹ a novel occupancy-driven lighting control system that aims to reduce energy consumption while simultaneously preserving the lighting comfort of occupants. By leveraging the fine-grained occupancy information estimated by existing WiFi infrastructure in a nonintrusive manner, WinLight computes an appropriate dimming command for each lamp based on a novel lighting control algorithm. The experimental results demonstrate that WinLight achieves 93.09% and 80.27% energy savings compared to static scheduling lighting control scheme and passive infrared (PIR) sensor-based lighting control scheme while guaranteeing the personalized lighting comfort of each occupant.

Table 1 summarizes the comparison results of the proposed framework with different technologies proposed in literature. The overall kWh saving is considered for this analysis. It can be clearly observed that the maximum energy efficiency of 90% is achieved by the proposed framework. The reason lies in the fact that the different implementation in the literature either considers replacement of load appliances with energy-efficient loads or deploys occupancy based load management controllers in isolation. The proposed work not only combines both, by in fact it also utilizes renewables as a distributed generation source to achieve energy sustainability as well.

3 | METHODOLOGY: COMPONENTS, ENERGY TECHNIQUES, AND ICT TOOLS

A three-layer framework is proposed to achieve active energy saving is shown in Figure 2. There are two dimensions in the proposed framework. In the vertical dimension, the key functions to achieve energy efficiency starts with the building simulation model estimations.

The simulation analysis of the building envelop provides a good estimate to determine yearly energy requirements and the peak energy required to achieve ambient room condition in all weathers.¹⁰ An isolated model of the building is generated in the Autodesk Ecotect software to check for the effective thermal variations in the said office due to its particular locality in the building. Then, this isolated model is used in simulation with weather parameters to approximate the actual temperature variations in the office and the heating/cooling requirement for comfortable conditions. The

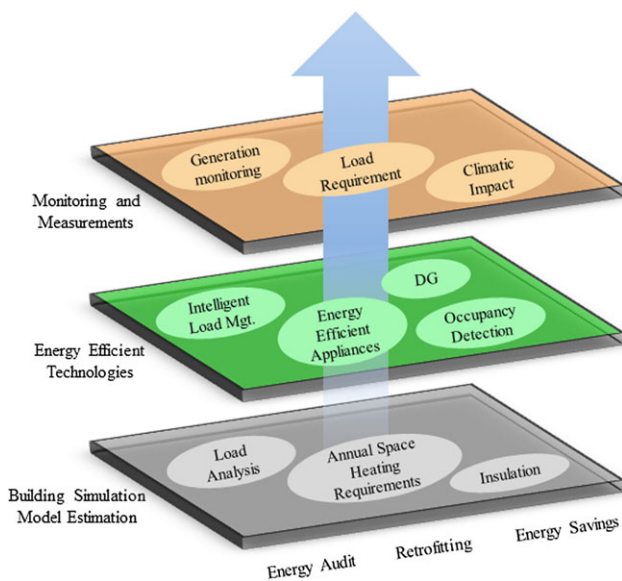


FIGURE 2 System components and methodological flow. DG, distributed generation

building model is put to test under the annual weather conditions of the local area. There is no encapsulation used in the initial simulation results. Therefore, the next step uses various insulation types for varied thickness of envelope of polystyrene foam. Based on the simulation analysis, the base load is assumed to be around the peak generation requirement for annual space heating requirement, which was found to be 1.5 kW. The area under consideration is to be used as a multioffice location, which includes a faculty office, a liaison office, and the record keeping office. Thus, it will serve as deskbound location for 15 persons along with their computer stations. These persons and the computing equipment serve as the heat-generating bodies, which form the active load. For approximate air conditioning load calculation, ASHRAE standard is followed, which, along with the operation loads requirements, poses the power requirement of 2.5 kW. The overall electrical load requirements therefore becomes 4 kW. In order to size the generation system, around 33% increase in the generation is considered to account for the conversion losses and the peak load; therefore, the final generation requirement was calculated to be 6 kW.

The energy-efficient technologies layer consists of the various active energy conservation techniques including, an upgradation to energy-efficient appliances, photovoltaic (PV) system as a distributed energy source (distributed generation), intelligent load management, and occupancy detection and localization controllers. The implementation of load management algorithm in smart home scenario using involves internet-of-things-based ICT architecture.^{11,12}

The monitoring and measurement layer consists of data logging devices to observe the overall system behavior and based on the measured data generates control signals for the controllers to achieve energy conservation and increase the energy efficiency as well.

The second dimension of the framework is categorized based on the steps needed to guide each of the three layers to achieve energy efficiency. Energy audit phase involves the preanalysis of loads and the determination of system size. Retrofitting phase involve the transformation of existing system elements into energy-efficient components. The energy-saving phase determines the overall energy savings that can be achieved through the proposed transformations. After the thorough analysis, the overall system requirements were laid down, which consists of the following main components/subsystems:

1. 6KW grid-tied mono crystalline PV-based energy generation system to meet the load requirements as a primary source,
2. Solar data logger device to measure peak generation possibility during the sun hours,
3. Selection and installation of energy-efficient loads (lighting and air conditioning),
4. Embedded hardware for occupancy detection and localization,
5. Intelligent load management controller for efficient use of generated energy.

In order to understand the overall system, it is necessary to discuss each component in details in the subsequent sections.

3.1 | Source selection

One of the key aspects of very low-energy buildings is power generation by renewable resources so the selection of power source is dependent upon the local atmospheric conditions. The test site is based in Peshawar so the technology of choice was easily the solar PV generation. The accessories for deployment of PV panels are readily available in Peshawar and there is great variety of tools available from a number of vendors and manufacturers. Motivated by these reasons, a solar PV system (shown in Figure 3) was deployed at the roof of Abasyn University to provide for the energy requirements of the system.

Two arrays of PV panels were installed on the roof where each panel generates 250 watt at peak generation hours and each array comprising of 12 panels. Therefore, each array generates 3000 watt at peak hours and the total generation is 6000 Wp or peak-watt. Individual panels were made from high quality monocrystalline silicon cells and comprise of 6 of these cells in series configuration. Monocrystalline was preferred over others due to its better quality, efficiency, and wide range of temperature withstanding capability.¹³ The PV panels were fixed to ground via galvanized mounting fame, which is strong enough to withstand wind speeds up to 100 km/h. The galvanized frame is rust-proof and supports PV panels at a 29-degree fixed tilt with respect to ground, facing south.

Two sets of Axpert 3 kW VMII solar inverters were installed, with each connected to a string of 12 PV panels thus each module converting 3000 W of dc power to ac power. Both inverters were identical as they are rated for 3000 W/Unity power factor at 230 volt-ac. The system deployed was battery-less and grid intertie, which saves substantial costs. Basically, these modules not only perform the inversion process but some other intelligence is there as well, eg, there is an intelligent voltage stabilization function in it which regulates the output voltage around 230 V, although the fluctuations from input side are quite significant before sunset and after sunrise. There is also a maximum power point-tracking function in



FIGURE 3 Front array of installed photovoltaic system at Abasyn University

it, which gives maximum possible output power regardless of load, based on proximity algorithm.¹⁴ Another desirable function is that of charge controller, which prevents overcharging and draining (in case a battery is added to system for storage), protects against overcurrent, and overvoltage conditions. It also has intelligent function of operating between grid and PV supply where it preferably operates at solar energy but automatically switches to grid in case of low power or fault occurrence. It also has a power factor correction function, which helps in improving the dominant inductive or capacitive load.

3.2 | Solar data logger

The performance of the PV panel greatly varies from its rated values due to its assembly and the demography of the site where it is deployed. The measurement of solar radiation at a certain location requires physical presence at the installation site, and by means of a pyranometer, the radiation pattern can be recorded.¹⁵ This, along with the surface temperature, can be used to estimate the power that can be generated by the PV panel at any instance of time. Accurate measurement devices to record solar radiation are available, but they are usually very expensive. Furthermore, the integration of such devices sometimes becomes very cumbersome.¹⁶ The recording of surface temperature of objects that are placed under the sunlight also requires separate measurement devices. Furthermore, the limitation of physical presence of the person to record the values is a cumbersome task. One solution that exists is to address this problem is using meteorological satellites, but real-time data acquisition through such means requires high cost in the form of satellite payload. Most of the data regarding the solar radiation pattern for specific locations is either statistically generated or made available for previous years in the form of weather data files. Furthermore, there exist no devices that can record actual readings of voltage, current, and surrounding temperature/surface temperature of the PV panels installed at remote sites and can transmit it to server using wireless technology.

This compelled the research team to develop a device, which is aimed to measure and remotely communicate real time values of measured voltages, currents, and surface temperatures of the PV panels. This has been achieved by designing an electrical circuit based that is connected between the generation source and the load. The solar data logger device measures the voltage, current, and temperature values of the PV panels and transmits the data over internet using free hosting channels. The connection diagram of various modules used in the solar data logger device is shown in Figure 4.

The complete circuit diagram of the device is depicted in Figure 5. Voltage levels from the PV panel are measured using a simple voltage divider. Hall-effect-based sensor is used to measure the current drawn by the connected load on real-time basis. The dedicated temperature sensor then measures the surrounding temperature and, together with the voltage and current values, sends it to the microcontroller. The microcontroller then appends the data with the time stamp and, through a Zigbee module, transmits the data over the internet. At the server site, the data is retrieved from the web server using a predefined retrieval key. The packet size of the data is around 2 kB and time resolution of the measured values can vary from a minimum of 1 second to any desired resolution.

The time resolution of 2 minutes was selected, meaning that the microcontroller sends data for transmission after every 2 minutes. The same data can also be used for the analysis of PV reliability and PV aging; however, such analysis does

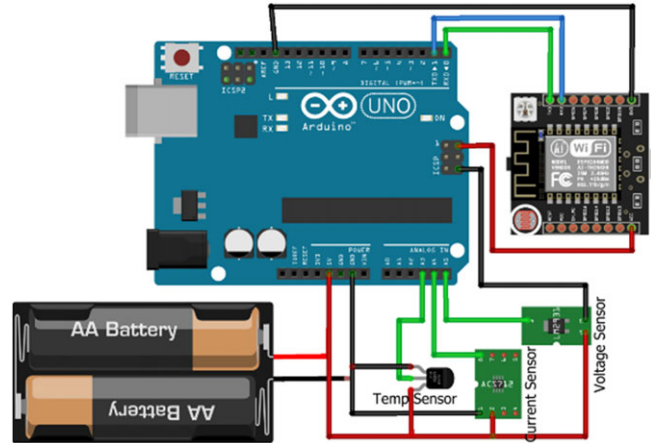


FIGURE 4 Connection diagram of solar data logger

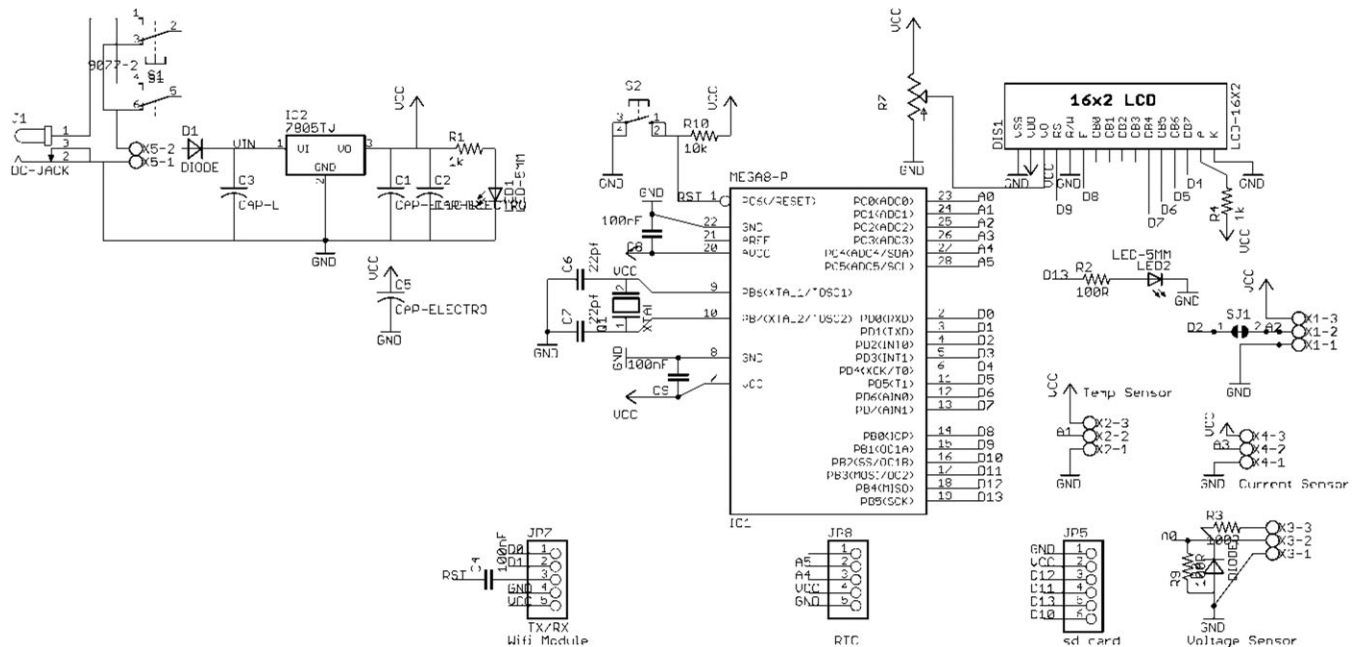


FIGURE 5 Complete circuit diagram of the solar data logger

not fall into the scope of present research. A possible extension of this research can be to extend the functionality of the device to record air flow, water flow, and thermal effects at remote sites and, with mass deployment across the country, this device can be used to identify feasible sites for renewable energy harvesting. Moreover, with the help of the same device, PV reliability analysis can be done on real-time value, where the PV panels remain deployed at the remote locations.

3.3 | Cooling/heating equipment

Instead of going for separate devices, current technologies of air conditioner offer dual mode operation, ie, they have cooling and heating functions. Amongst the available air conditioners, there are different brands offering different features and energy-efficient products. Therefore, the product selected also needed to be energy efficient.

Therefore, GREE® DC inverter air conditioner was selected as it features multiple mode operation including the heating and cooling modes and very high energy efficiency ratio of 3.24, which is due to its unique DC inverter technology. This technology saves a lot of energy as compared to other energy-efficient split air conditioners available by giving energy at higher frequency to compressor. This not only fulfills the required energy consumption within the constraints but also offers cooling at lower energy expense than the one considered for the calculations.

3.4 | Interior lighting requirements

The test site considered as an office for 15 persons, so it requires an ample amount of lighting for doing different tasks. The office illumination standard is nearly 50 foot-candle or 500 lumens/m² for normal office work with PCs, etc. The model office is approximately 60 m² in size (71 m² if walls area is included) so a net amount of 30 000 lumens has to be provided for the office. The commercially available energy-efficient LED lights give out about 100 lumens/watt, which gives around 300 watts of essential lighting load using LED lights. A total of 22 energy-efficient LED lights were installed at the office to supply the required illumination. The electrical load of lights sums up to slightly greater than 300 watt. Individual lighting unit is a high-intensity LED lighting module of 14-watt power consumption and is mounted in a circular housing for evenly spreading the light.

3.5 | Occupancy detection

Presence detection using micro-electromechanical system (MEMS) thermal sensors is an intelligent way of controlling and managing the loads in a building. Intelligent load management under constrained energy availability is a way of extending the backup and thereby reducing the installation size of renewable energy sources like solar energy and wind energy systems in buildings.^{17,18} This is important in terms of reducing the cost of initial installation of such systems. Many times, majority of the loads in the buildings can be categorized as critical loads and noncritical loads. However, some of the loads may fall in both categories depending on the comfort level and convenience of the user. Depending on the availability of a person in a room, the loads can be turned on or off.

The occupancy detection and localization is achieved by employing Omron's D6T-44 L MEMS thermal sensors^{19,20} and using Arduino Uno board. These are high-sensitivity sensors that enable detection of stationary human presence. These are high-precision area temperature detection with low cross-talk field-of-view (FOV) characteristics along with superior noise performance and digital output. These readings are used and, based on a threshold level, we could assert whether a person was present or not. D6T-44 L-06 has sensor chip arrays of 16 channels (4x4). Each channel corresponds to a pixel and measures temperature independently. In the FOV of the sensor that includes all the pixels, whenever an object appears, the temperature of corresponding pixel changes. By mounting the signal processing circuit closely to the sensor chip, a low-noise temperature measurement is realized. Note that the occupied area in FOV becomes smaller with increasing distance and the background temperature prevails, as shown in Figure 6. Therefore, for detecting human beings, the application will be limited to close range when the detection programming scheme only judges by temperature value. To extend the detection distance, improvements to the judgment accuracy can be made via software programming, considering time change, heat source location, and human-being movement. The output from one of the occupancy detection hardware is shown in Figure 7. It is worth mentioning that the thermal sensor behaves differently with change in temperature. The sensing range gets affected with change of mode of air conditioning in summers and winters. For example, in summers, when air conditioning operates in cooling mode, the heat sensors can easily capture the heat print of the human body with respect to the surroundings objects with high resolution. However, when the air conditioning runs in heating mode, then the heat impression of human bodies get blends with the surrounding objects with a very narrow temperature difference. As a result, the occupancy detection encounters big error margin. This issue can be rectified by operating the controller in two distinct modes. In the heating mode, the significant digits of the sensor reading plays crucial role and the controller is made sensitive to respond to the minor changes in least significant digits.

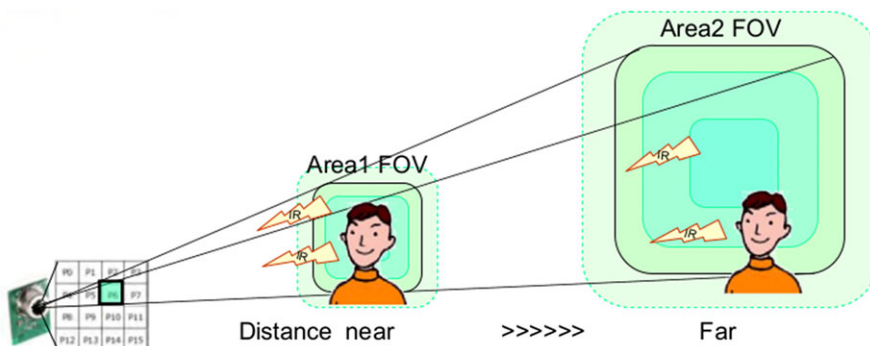


FIGURE 6 Changing factor of measurement by distance. FOV, field of view

16.8	18.4	19.8	21.3
15.2	15.7	18.4	19.6
12.8	14.6	17.6	19.1
12.5	13.0	14.3	22.8

FIGURE 7 Sensed temperature outputs of sensor hardware with color coding

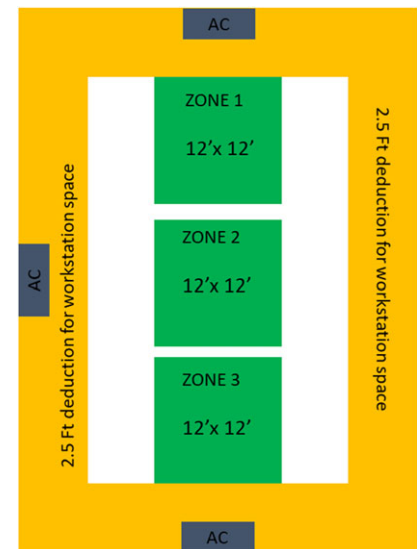


FIGURE 8 Zone distribution of the building envelop

In this research, the building envelop was divided into three zones and for the maximum floor coverage, three sensors are installed at different locations which continuously provided the temperature readings of all the locations in separate 13.4 m^2 (144 ft^2) square grid. Figure 8 shows the zone wise distributions of the building envelop, where each sensor covers the floor area of respective zone. It is worth mentioning that 0.76 m (2.5 ft) space at each edge is intentionally left with no sensor coverage due to the fact that this space shall be occupied by the stationary workstations. The white space in Figure 8 shows the area where no coverage area of the thermal sensors. Perhaps this is the only limitation of the current hardware, which can be easily rectified by deploying additional sensor hardware, or by filling the uncovered sensor area with stationary objects like printer and water dispenser, so as to avoid long term presence of moving objects.

3.6 | Intelligent load management algorithm

This research uses PV-based electrical energy generation system, which is designed to meet the peak load demand of the building envelop. The amount of generated energy varies with time due to the change in solar azimuth. This means that the energy requirement during activity hours may not be fulfilled by the generation system at all times. The main task of the intelligent load management algorithm is to manage air conditioning loads based on occupant behavior.²¹ Occupant behavior is used in predicting the energy use of a building in a way that occupants interact with building features. This helps in estimating building energy use and the impact on energy demand by changing behaviors. Our

TABLE 2 Various scenarios for “intelligent load management”

Available Generation Capacity	Occupancy			Decision (Duration is 15 minutes)
	Zone 1	Zone 2	Zone 3	
1.2 KW	✓	-	-	Activate AIR CONDITIONING in Zone 1.
	-	✓	-	Activate AIR CONDITIONING in Zone 2.
	-	-	✓	Activate AIR CONDITIONING in Zone 3.
	✓	✓	-	Switch AIR CONDITIONING between Zone 1 and Zone 2 at an interval of 15 mins.
	-	✓	✓	Switch AIR CONDITIONING between Zone 2 and Zone 3 at an interval of 15 minutes.
	✓	-	✓	Switch AIR CONDITIONING between Zone 1 and Zone 3 at an interval of 15 minutes.
	✓	✓	✓	Switch AIR CONDITIONING among all the three Zones at an interval of 15 minutes.
	-	-	-	Activate AIR CONDITIONING among all the three zones only once at an interval of 15 minutes and then deactivate it.
2.4 KW	-	-	-	Activate AIR CONDITIONING in two zones at a time. Repeat the schedule for all possible combinations only once at an interval of 15 minutes and then deactivate it.
	✓	✓	-	Activate AIR CONDITIONING in Zones 1 and 2.
	-	✓	✓	Activate AIR CONDITIONING in Zones 2 and 3.
	✓	-	✓	Activate AIR CONDITIONING in Zones 1 and 3.
	✓	✓	✓	Activate AIR CONDITIONING in two zones at a time. Repeat the schedule for all possible combinations at an interval of 15 minutes and then deactivate it.
3.6 KW	-	-	-	Activate AIR CONDITIONING in all zones for an interval of 15 minutes only once and the deactivate it.
	✓	✓	✓	Activate AIR CONDITIONING in all the three zones.

task is to manage the energy supply to the whole building envelope on the basis of available energy generation. Various energy management scenarios are created, on the basis of which we can control our air conditioning units based on the available energy. The detailed scenarios are discussed in Table 2 where the cases are made for following three categories of produced energy:

- When energy generation is less than 1.2 KW;
- When energy generation is in between 1.3 to 2.4 KW;
- When energy generation is greater than 2.5 to 3.6 KW.

The research hypothesis considers three different scenarios based on the maximum available power generation by the PV source, ie, 1.2 KW, 2.4 KW, and 3.6 KW, as shown in Figure 9. At generation of 1.2 KW, only one zone can be connected to the power grid. At 2.4 KW, two zones can be connected to the generation supply, while 3.6 KW or above generation is enough to meet the energy load requirements of all three zones. The controller checks the power generation level first. If the power generation is equal to 1.2 KW, a single zone having an occupant count will be connected for the respective period of time. If the generation is between 1.2 KW and 2.4 KW, then based on the occupant count, two zones will be supplied with electricity. For 3.6 KW, all zones will be powered on for the occupants. When there are no occupants in any zone with power generation of 1.2 KW, each zone will be powered on for a respective period of time and then turned off until occupancy takes place in any zone. For power generation less than 2.4 KW, two zones (the cases which have been discussed earlier) will be powered on for a respective times and turnoff afterwards. In case of 3.6 KW, all zones will be powered on for respective times and then turned off until the zones are occupied. In case if there is no on-site power generation, eg, in dark clouds or rainy weather, then energy will be taken from the grid. In case of nonavailability of the grid electricity, the backup generator shall act as an energy source.

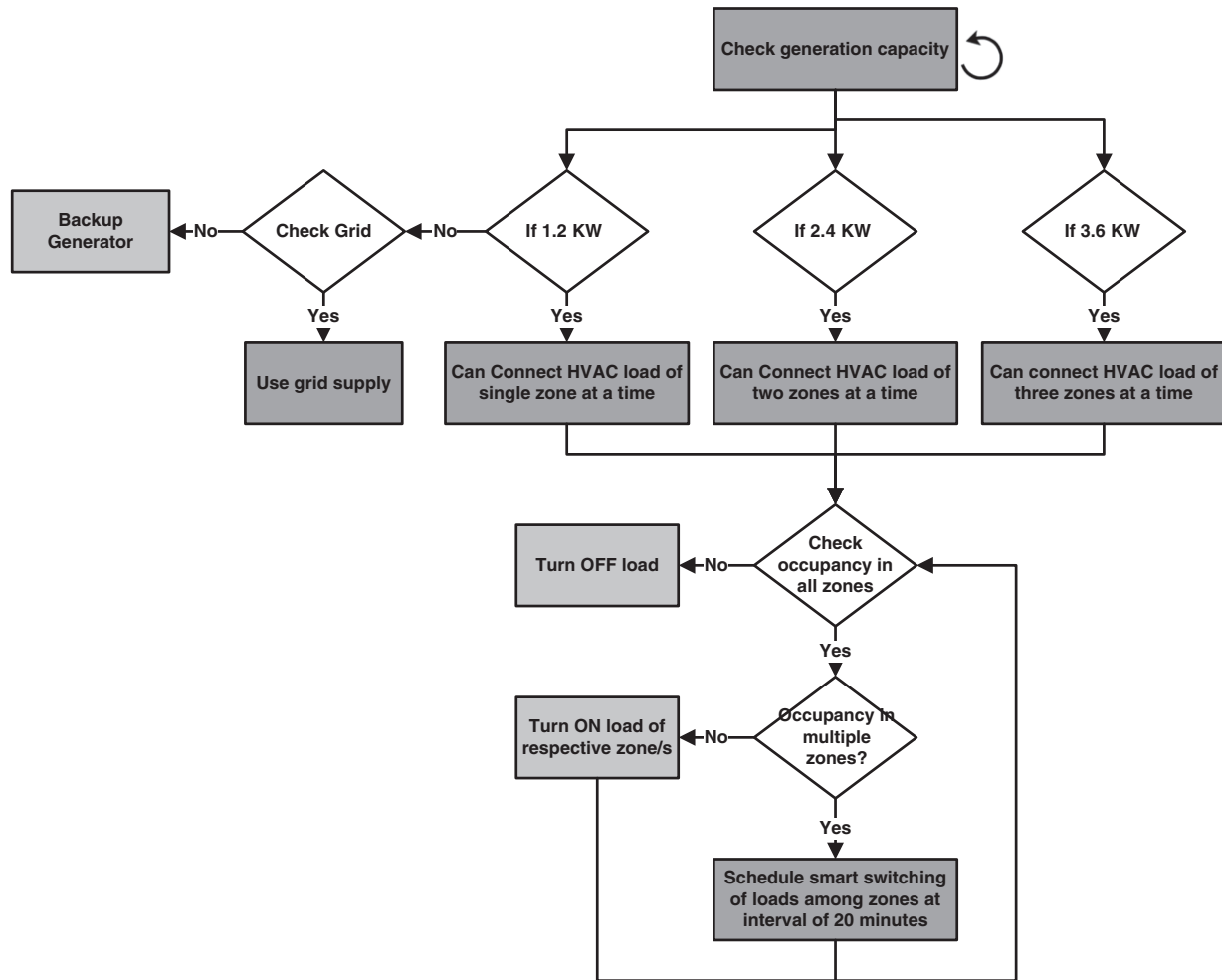


FIGURE 9 Flow chart of intelligent load management algorithm

4 | RESULTS AND DISCUSSION

4.1 | Cooling load

The system component chosen to fulfill the HVAC requirements is a 1-ton DC inverter air conditioner as it can cool, ventilate, and heat the facility it is installed in. Its multiple modes and lower power consumption than conventional split air conditioners made it an ideal choice for fulfilling the HVAC requirements. To completely satisfy the demands, three of these units were installed in the model building.

The graph in Figure 10 shows the actual power consumed by the DC inverter air conditioner unit installed at the facility. Start of graph corresponds to 7:50 AM in the morning and end corresponds to 5:11 PM in the evening. In the beginning, it operates at full cooling capacity, thus correspondingly consuming maximum power in the cooling cycle. After it has cooled the room down to required temperature, the air conditioner's cooling stabilizes and it comes down to low-power mode where it consumes almost half the power and stays in this mode for quite a long duration. This mode is a unique feature of DC inverter technology that keeps cooling at very low power instead of completely shutting off the compressor and then switching to full capacity when required, thus consuming more power in frequent switching between cooling and rest modes. In the aforementioned graph, the peak's amplitude depends upon the difference of temperature between outside and desired temperature set on air conditioner. Higher the difference in temperature, greater the power consumption, and thus, correspondingly, the peak is higher. Similarly, the length of intervals of high-power mode and low-power mode depends upon the temperature difference; higher temperature difference corresponds to longer high-power interval and shorter low-power interval, while lower temperature difference enables low-power mode to operate for longer duration.

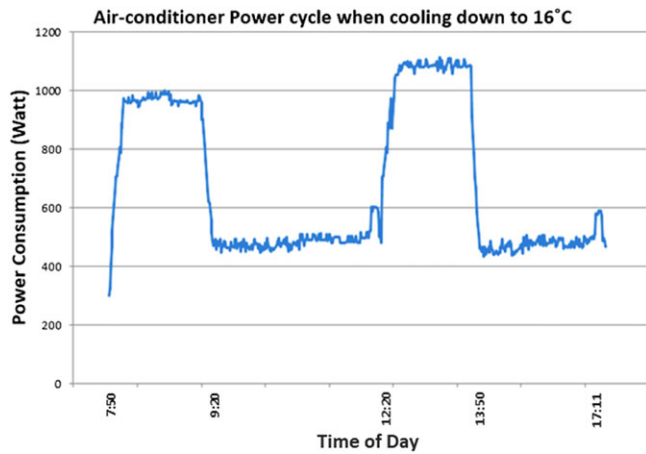


FIGURE 10 Air conditioner power cycle when cooling down to 16°C

Thus, during hotter days, higher peaks and lengthy high-power intervals mean higher power consumption and other days to have significantly low power consumption. Tables 3 to 5 shed some more light on actual power consumption at different temperature set.

	Activity	Time (minutes)	Power (watts)
CYCLE 1	Start-up period	20	800
	Room cooling period cycle1	90	1200
	AC getting to low-power mode/Stabilization	10	800
	Low-power mode	180	500
CYCLE 2	Recooling stabilization	20	800
	Room recooling period	90	1200
	AC getting to low-power mode/Stabilization	10	800
	Low-power mode disconnected in the end	180	500

TABLE 3 Approximate periods of power consumption for ac cooling room down to 26°C from 40°C

Average power consumption for the whole period = 750 watt (app).
Abbreviations: AC, air conditioner.

	Activity	Time (minutes)	Power (watts)
CYCLE 1	Start-up period	20	600
	Room cooling period cycle1	30	1100
	AC getting to low-power mode/Stabilization	10	700
	Low-power mode	240	500
CYCLE 2	Recooling stabilization	20	650
	Room recooling period	30	1150
	AC getting to low-power mode/Stabilization	10	700
	Low-power mode disconnected in the end	240	500

TABLE 4 Approximate periods of power consumption for ac cooling down to 26°C from 35°C

Average power consumption for the whole period = 580 watt (app).
Abbreviations: AC, air conditioner.

	Activity	Time (minutes)	Power (watts)
CYCLE 1	Start-up period	15	600
	Room cooling period cycle1	30	800
	AC getting to low-power mode/Stabilization	10	600
	Low-power mode	120	300
CYCLE 2	Recooling stabilization	15	600
	Room recooling period	30	750
	AC getting to low-power mode/Stabilization	10	450
	Low-power mode disconnected in the end	120	300

TABLE 5 Approximate periods of power consumption for ac cooling down to 26°C from 30°C

Average power consumption for the whole period = 420 watt (app).
Abbreviations: AC, air conditioner.

4.2 | Actual solar PV generation

The actual output of the PV system is shown on daily (Figure 11) and weekly bases (Figure 12). First, the daily power generated by PV system is plotted against the corresponding day, and then the same is done with the daily energy generated by system. The graphs show the average values for the day as it fluctuates between zero and a few thousands following the pattern of sunlight. Therefore, each day has a very large set of power values recorded every minute, with diminishing values near sunrise and sunset. The value representing each day is the average of all those recorded data and is good for comparison when calculating monthly and annual yields of the system.

The first full week or 7 days show a quite low output as compared to other days, which was due to dust that had settled on the PV panels for over a month. The PV panels were cleaned on September 30 and, consequently, the output increased as is evident from the corresponding sharp spike in Figure 13. The daily output also fluctuates with cloud cover, smog, rain, nearby human activity, etc, as depicted in Figure 14.

4.3 | Effect of dust cover on PV panels generation

To study the effect of dust settling on the panels on the PV system's generation, the panels were not cleaned during the first week of the system's installation and values were monitored for the whole week. That week was termed as week0 and

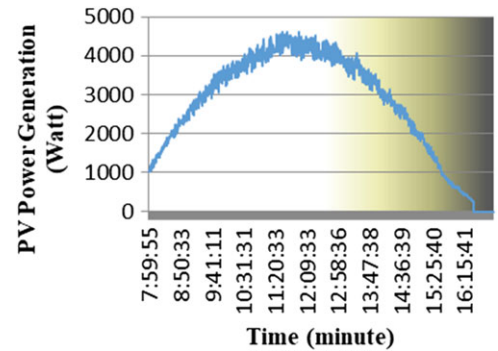


FIGURE 11 Hourly power generation of photovoltaic (PV) on October 1, 2018

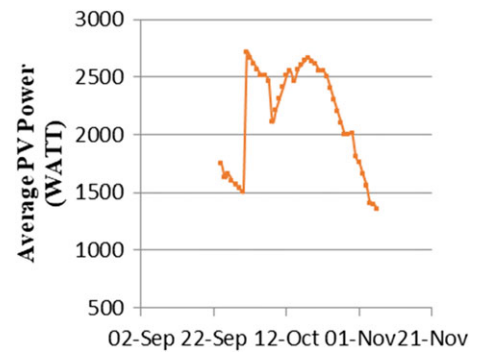


FIGURE 12 Average daily electrical power generated by photovoltaic (PV) system

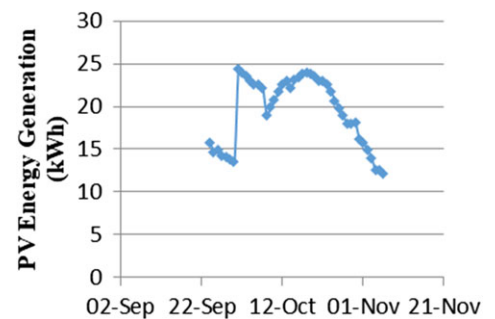


FIGURE 13 Daily electrical energy generated by photovoltaic (PV)

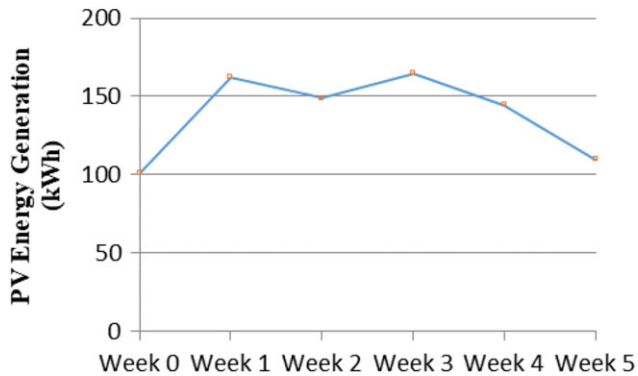


FIGURE 14 Weekly energy generated by photovoltaic (PV)

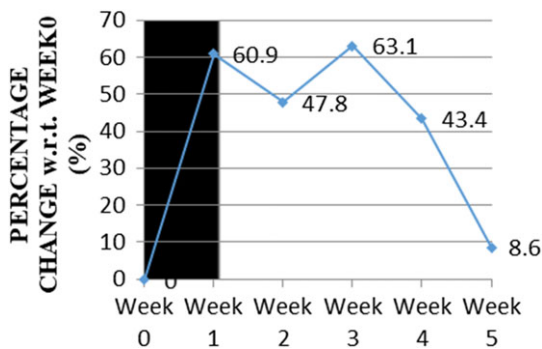


FIGURE 15 Clean versus unclean photovoltaic panel's generation comparison

next week was week1 and so on; to differentiate it from other weeks, it is shaded in black area in the graph in Figure 15. The panels were cleaned on September 30 and a huge change was observed on October 1 as compared to previous week as evident in daily and weekly generation graphs. The next few weeks shown greater performance before unprecedented levels of smog covered the city. In the following graph, the weekly output of system is compared with the week0 of its operation with percentage change w.r.t. week0 on vertical axis.

The output of panels increased to more than 60% in the cleaning week and then week2 showed nearly 50% improvements over week0. Similarly, week3 and week4 were 63% and 43% better than week0, respectively. The graph clearly shows that in subsequent weeks the output increased to about 50% for clean panels as compared to dusty ones. Therefore, it is imperative to clean the PV panels on regular basis otherwise the losses are substantial and may amount to more than 50% power and energy loss in the production and thus rendering the mismatch in system design.

4.4 | Effect of smog on PV panels generation

In recent times, due to rapid industrialization and urbanization, deforestation for land and industrial uses, uncontrolled pollution swells, and other such unpleasant phenomena, the smog has developed as a major player in local environment. Not only is it adversely affecting overall health and life of the populace, but it is also interfering with weather, eg, polluting the air, increase in acidity of rains, diffused sunlight, etc.

One critical aspect of the smog is hindering the usual sunlight reaching the earth surface, which results in diffused and weak light for use of PV panels. Renewable energy resources especially solar technologies were gaining momentum in recent years due to uncertainty over conventional fossil fuels, but all the solar technologies require sunlight at its maximum to operate efficiently. Thus, smog is greatly interfering with solar technologies and, with PV technologies having efficiencies in the range of 15% to 20%, the losses are great.

During the operation of the system installed at model building, a smog cover interfered with regular working of the plant during the last week of the October, but situation worsened in the early November until rainfall. The smog cover was sometimes dense enough to block major portion of sunlight and severely affect the output of PV, as shown by the recorded values of the graph in Figure 16. During the first week of November or week5, it can be seen that output has fallen to almost the same levels as the week0, ie, dusty panels. The week is highlighted in the graph as light blue portion of

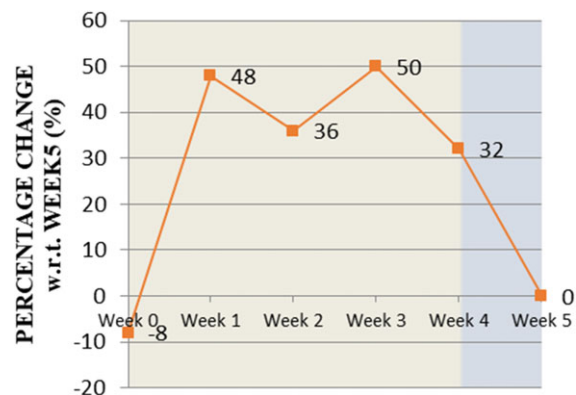


FIGURE 16 Photovoltaic panels generation comparison

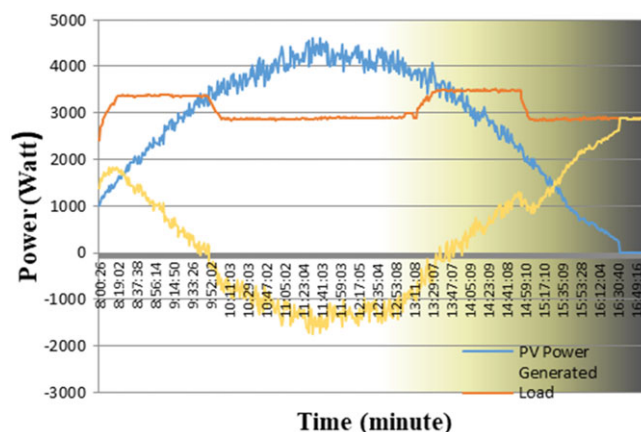


FIGURE 17 Comparison of photovoltaic (PV) power generation, load, and power taken from grid

the area and shows that more than 30% of the generation is lost due to smog. These graphs not only provide information about the decreased output of the PV but can also help in formulating a method of quantifying and monitoring smoggy conditions, eg, percent decrease in PV output, erratic generation patterns, etc.

4.5 | Photovoltaic generation versus load

The chart in Figure 17 shows a comparison of the power generated by PV as blue curve and actual power consumption at test site in red. The green curve shows the power taken from grid when solar power is not enough to support the full load. As it can be seen that at start of the day, PV generation is low and, thus, major power flow is from grid. With time, PV generation increases and, thus, dependence on grid decreases and, around 10:00 AM, the power flow from grid stops. Then, there is period of high generation from PV where PV power is surplus and can be supplied back to grid. Around 1:30 PM, PV's generation again falls below load requirement until around 4:30 PM, which PV generation is zero and there is complete dependence on grid.

5 | FINANCIAL ANALYSIS

One of the key points in project feasibility analysis is the estimation of payback period of the project.²² This assessment is valuable in checking whether the project would return the costs it would incur and thus would be profitable or not. For decision making, payback, and cost, benefit analysis can be used for evaluation of multiple competing projects, which are all profitable. For these analyses, different parameters like capital expenditure, taxes, running costs, benefits, and estimated system life are taken into account.²³ The benefits are evaluated and given some monetary value; then, these are weighed against the costs over time and declining condition of the plant to do break-even analysis, which gives the payback time. These analyses are furthered for the overall system benefit calculation and unit price calculations, etc. Table 6 states the annual generation figures and the overall cost of the system.

Annual Cooling/Heating Load (kWh)	1584.6
Annual Energy Requirement (kWh)	10 484
Required/Actual Solar PV system (kW-Peak)	6240
Estimated Generation of PV system per annum (kWh)	11 620
Initial Cost of System Deployment (\$)	7360
Annual Maintenance Costs (\$)	770

TABLE 6 Generation estimates and system costs

Abbreviations: PV, photovoltaic.

Annual cooling/heating loads for all the insulation coverage were taken from the simulation results. The annual energy requirements for other office activities were estimated and both loads combined including system losses are shown in the second row of the Table 6. Due to limitations in capacity of commercial solar PV modules and lower per watt cost of bigger modules, an exact supply and demand match was not possible. Therefore, each scenario was virtually provided with a system feasible according to its requirements. Since the systems would have generated energy more than the load needs, actual outputs of the PV systems are also given. This, also, is the criterion of the benefit and payback analyses of the systems. Then, further down the table, the initial cost of the system is given, which includes all the costs of PV system installation, energy-efficient load appliances, and installation of intelligent load management controller and other accessories.

In order to perform the payback calculations, the previously given financial information is utilized. The average solar system life is 25 years and it is warranted that it will not fall below 1% per year, which is incorporated into the analysis as panel degradation factor. The electric unit price is taken to be 0.18\$, which is the average value currently charged by the power distribution company for the commercial utilities. The average increase in unit price is calculated from the inflation statistics provided by the State Bank of Pakistan²⁴ and it is applied for the whole period of study, ie, 25 years. This information is same for both systems and Table 7 summarizes this information.

For competitive analysis of the whole project, the financial information for the framework is summarized in Table 8. However, it should be noted that all the costs are rounded to nearest unit dollars. The payback period of the project is 6 years. To be more precise, soon after the completion of fifth year, the project will turn all profitable for the subsequent plant life, ie, 19 years. This implies that the overall system cost, ie, 11 980\$, which is the sum of costs for system deployment (7360\$) and the annual maintenance cost for 6 years (4620\$) is recovered during the first 6 years of the deployment, thus providing the breakeven point. By the end of project life cycle, not only the costs would have been recovered, but also an approximate net profit of 48 382\$ will have come out of the system. Another feature considered in the comparative analysis is the levelized cost of energy, which shows an estimate of base price for unit production of the plant and is one of the best features of a solar PV plant as compared to all other electricity generation systems whose unit price are mainly governed by higher running and maintenance costs and thus are fluctuating with time and are uncertain over lengthy periods of time.²⁵ Therefore, solar system has significantly lower uncertainty and lower risk involved for its period of operation, which is quite long and stable.

Life of solar system	25	Years
Average Electric Unit Price	0.18	\$
Average Increase in unit price	4%	Per annum
Panel Degradation Factor	1%	Per annum

TABLE 7 Financial information for payback calculation

Project Costs over full project cycle (\$)	26 580
Net Earnings over full project cycle (\$)	48 382
Net Present Value of Net Earnings of Project (\$)	18 690
Internal Rate of Return	22%
Payback Period	5 to 6 years
Levelized Cost of Energy (\$)	0.10

TABLE 8 Payback analysis

6 | CONCLUSION AND FUTURE WORK

This research has considered wide variety of fields ranging from renewable resources, electrical load optimization, and load forecasting to pollution mapping to conserve energy in commercial buildings. The diverse range of considerations has opened doors to many areas and, thus, this project can be further explored into many directions and disciplines. There was a high loss of energy in conversion of electrical energy from direct current (DC) to alternating current (AC) although very efficient equipment was used. This shortcoming can be overcome by using DC loads and decreasing AC loads in the system. One step is to use DC lighting system whose savings are substantial for larger utilities. Then, there is space-heating equipment, which is the most power consuming and lossy component of the system and can save huge amounts of energy if it can be connected to run on DC system.

The data-logger device designed for the system can be enhanced to record other parameters like light intensity, power/energy consumption and generation, temperature, maximum power point, wind speeds, etc. A utility can be developed for comparative and analytic assessment of the monitored factors. Thus, it will not only serve as data recording equipment but also a potential estimator for renewable technologies. An increase in smog in recent times has been observed and currently its measurement is difficult. The data-logger device mapping can be used for this purpose as well. It is observed in the solar PV generation that it can be increased to around 20% of the current generation by using solar tracking technique, which involves movement of the panels to always face the sun. The values given are supported by the intensity measurements done at the test site.

To maximize the PV output further, solar concentrating techniques can be used, which utilize reflecting mirrors and mirror/lens combination for increasing the sunlight falling on PV panel, thus increasing its generation around 30%. It also increases PV modules' temperature, which reduces efficiency, but an overall gain can be achieved by adjusting the factors for maximum productivity. Load forecasting techniques can be employed for closely matching generation with the load requirements to save potential costs of generating system. Additionally, power-saving schemes can be helpful in saving energy and use of both techniques can further lead to substantial saving of costs and energy. In addition, source-load matching techniques for maximum power transfer can be adopted for avoiding losses.

It was observed that PV modules' efficiency is severely affected due to dust cover of even a week and requires consistent human effort for cleaning and maintenance. In this era of automation, it proves to be a tedious job and, thus, an automatic cleaning system can prove to be beneficial, but it should be designed to take minimal power thus with minimum effect on costs and savings. The commercially available power conditioning units are versatile, but very costly and have limited connectivity and monitoring options. These units are locally assembled and their parts including the motherboard are readily available. Other cheaper units are also available with limited functionality but versatile connectivity and monitoring options. Therefore, a combination of available parts of costlier units with motherboard of cheaper units can be explored for commercial and research purposes.

ORCID

Affaq Qamar  <https://orcid.org/0000-0002-4350-4677>

Javed Iqbal  <https://orcid.org/0000-0001-7747-8801>

REFERENCES

1. Foster R, Ghassemi M, Cota A. *Solar Energy: Renewable Energy and the Environment*. Boca Raton, FL: CRC Press; 2009.
2. Feist W, Pfluger R, Kaufmann B, Schnieders J, Kah O. *Passivhaus Projektierungspaket 2007*. Passivhaus Institut Darmstadt: 2007.
3. Heidari M, Majcen D, van der Lans N, Floret I, Patel MK. Analysis of the energy efficiency potential of household lighting in Switzerland using a stock model. *Energy Build.* 2018;158:536-548.
4. Raftery P, Li S, Jin B, Ting M, Paliaga G, Cheng H. Evaluation of a cost-responsive supply air temperature reset strategy in an office building. *Energy Build.* 2018;158:356-370.
5. Yun GY. Influences of perceived control on thermal comfort and energy use in buildings. *Energy Build.* 2018;158:822-830.
6. Labeodan T, Zeiler W, Boxem G, Zhao Y. Occupancy measurement in commercial office buildings for demand-driven control applications—a survey and detection system evaluation. *Energy Build.* 2015;93:303-314.
7. Yoganathan D, Kondepudi S, Kalluri B, Manthapuri S. Optimal sensor placement strategy for office buildings using clustering algorithms. *Energy Build.* 2018;158:1206-1225.
8. Li Z, Dong B. Short term predictions of occupancy in commercial buildings—performance analysis for stochastic models and machine learning approaches. *Energy Build.* 2018;158:268-281.

9. Zou H, Zhou Y, Jiang H, Chien S-C, Xie L, Spanos CJ. WinLight: a WiFi-based occupancy-driven lighting control system for smart building. *Energy Build.* 2018;158:924-938.
10. Borenstein S. The market value and cost of solar photovoltaic electricity production. Berkeley, CA: University of California Energy Institute; 2008.
11. Khan M, Iqbal J, Talha M, Arshad M, Diyan M, Han K. Big data processing using internet of software defined things in smart cities. *Int J Parallel Program.* 2018. 1-14.
12. Iqbal J, Khan M, Talha M, et al. A generic internet of things architecture for controlling electrical energy consumption in smart homes. *Sustain Cities Soc.* 2018;43:443-450.
13. Ren J, Lützen M. Selection of sustainable alternative energy source for shipping: multi-criteria decision making under incomplete information. *Renew Sustain Energy Rev.* 2017;74:1003-1019.
14. Ishigaya A, Kamiya N, Kubota Y, Yoshimura M. High-efficiency converter technologies for advanced air conditioner. Paper presented at: PCIM Asia 2017; International Exhibition and Conference for Power Electronics, Intelligent Motion, Renewable Energy and Energy Management; 2017; Shanghai, China.
15. Huang Y-C, Lee S-K, Chan C-C, Wang S-J. Full-scale evaluation of fire-resistant building integrated photovoltaic systems with different installation positions of junction boxes. *Indoor Built Environ.* 2017;27(9):1259-1271.
16. Raptis P, Kazadzis S, Psiloglou B, Kouremeti N, Kosmopoulos P, Kazantzidis A. Measurements and model simulations of solar radiation at tilted planes, towards the maximization of energy capture. *Energy.* 2017;130:570-580.
17. George B, Zangl H, Bretterkleeber T, Brasseur G. Seat occupancy detection based on capacitive sensing. *IEEE Trans Instrum Meas.* 2009;58:1487-1494.
18. Beltran A, Erickson VL, Cerpa AE. Thermosense: Occupancy thermal based sensing for HVAC control. In: Proceedings of the 5th ACM Workshop on Embedded Systems For Energy-Efficient Buildings; 2013; Rome, Italy.
19. Aftab M, Chen C, Chau C-K, Rahwan T. Automatic HVAC control with real-time occupancy recognition and simulation-guided model predictive control in low-cost embedded system. *Energy Build.* 2017;154:141-156.
20. Geiger J, inventor: Ams Sensors Singapore Pte Ltd, assignee. Non-contact thermal sensor module. US patent US9658109B2. 2017.
21. Liu X, Ivanescu L, Kang R, Maier M. Real-time household load priority scheduling algorithm based on prediction of renewable source availability. *IEEE Trans Consumer Electron.* 2012;58(2):318-326.
22. Numbi B, Malinga S. Optimal energy cost and economic analysis of a residential grid-interactive solar PV system-case of eThekweni municipality in South Africa. *Appl Energy.* 2017;186:28-45.
23. Tripathy M, Joshi H, Panda S. Energy payback time and life-cycle cost analysis of building integrated photovoltaic thermal system influenced by adverse effect of shadow. *Appl Energy.* 2017;208:376-389.
24. Hussain I. Banking industry concentration and net interest margins (NIMs) in Pakistan. *J Bus Econ Manag.* 2014;15:384-402.
25. Fan Y, Xia X. A multi-objective optimization model for energy-efficiency building envelope retrofitting plan with rooftop PV system installation and maintenance. *Applied Energy.* 2017;189:327-335.

How to cite this article: Qamar A, Iqbal J, Saher S, Shah AA, Basit A. Design of optimized energy system based on active energy-saving technologies in very low-energy smart buildings. *Trans Emerging Tel Tech.* 2019;e3691. <https://doi.org/10.1002/ett.3691>

COPYRIGHT NOTICE

This material is for personal research purposes only. Do not distribute any copies, electronic or otherwise.

Further reproduction of documents - including photocopying, scanning or forwarding by e-mail - is an infringement of copyright law.

This material may be subject to further copyright restrictions not outlined here.

Additional copies must be requested through the Information Resource Centre.

irc.irc.moe@ontario.ca

416-327-1247